All-Optical Payload Envelope Detection for Variable Length 40-Gb/s Optically Labeled Packets

Brian R. Koch, *Student Member, IEEE*, Zhaoyang Hu, *Member, IEEE*, John E. Bowers, *Fellow, IEEE*, and Daniel J. Blumenthal, *Fellow, IEEE*

***Abstract*—We demonstrate a new technique to all-optically identify the precise temporal locations and durations of the payloads of optical packets consisting of a variable length 40-Gb/s return-to-zero payload and 10-Gb/s nonreturn-to-zero label. The all-optically generated payload envelope signal can be used to erase the original optical label and rewrite a new label. The recovered payload envelope has 300-ps rise time and edge root-mean-square average jitter of 30 ps over a 10-dB dynamic range of input optical packet power. These numbers indicate that this technique enables the use of very short guard bands between payloads. The technique is demonstrated using optical semiconductor devices that are straightforward to monolithically integrate on a single chip.**

***Index Terms*—Optical packet switching, optical signal processing, sampled grating distributed Bragg reflector laser (SGDBR).**

I. Introduction

OPTICAL label swapping has recently been studied as an efficient way of packet switching in lower power data switched networks [1], [2]. In this technique, information is transmitted as packets using optical labels, which are used to route the packets to their next destination. At switching nodes, the label for each packet is recovered, erased, and rewritten in the optical domain. Label erasure and rewriting requires precise knowledge of the temporal location of the payload. The principle and experiment presented in this letter focus on this task, called payload envelope detection (PED) [3], which is defined as identification of the precise location and duration of the payload. Previously, we have demonstrated PED circuits based on optoelectronic clock recovery [3], [4] which had several nanoseconds rise times and ~150 ps of timing jitter. An all-optical PED circuit can potentially reduce the rise and fall times as well as jitter, showing promise to increase channel utilization due to reduced guard band duration.

In this letter, we demonstrate the first all-optical PED scheme for all-optical label swapping networks. Operation is based on a resonant laser with low Q-factor to remove 10-Gb/s nonreturn-to-zero (NRZ) optical labels, followed by a gain suppressed laser to generate envelopes of 40-Gb/s return-to-zero (RZ) optical payloads only. The PED signal has several bits rise/fall time due to the low Q-factor of the resonant laser. We analyze the relationship between the Q-factor of this laser and the rise/fall time of the signal. The fast rise/fall time and low jitter measured mean that very short guard bands are possible between labels and payloads. The scheme uses only optical semiconductor devices: a sampled grating distributed Bragg reflector (SGDBR) laser, a laser diode (LD), and a semiconductor optical amplifier (SOA). Characteristics of the PED signal including rise time, root-mean-square (rms) jitter, and amplitude are consistent over 10-dB input dynamic range.

Manuscript received April 27, 2006; revised June 20, 2006. This work was supported by LASOR award W911NF-04-9-0001 under the Defense Advanced Research Projects Agency (DARPA)/MTO DoD-N Program.

The authors are with the Electrical and Computer Engineering Department, University of California, Santa Barbara, CA 93106 USA (e-mail: koch@ece.ucsb.edu; huby@ece.ucsb.edu; bowers@ece.ucsb.edu; danb@ece.ucsb.edu).

Digital Object Identifier 10.1109/LPT.2006.881209

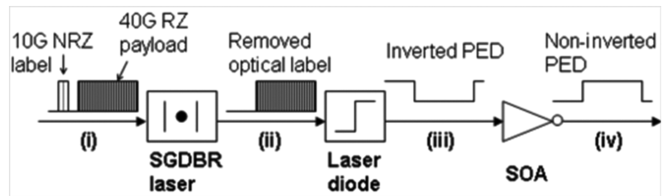

Fig. 1. All-optical PED operation principle.

II. Operation Principle and Experimental Setup

The all-optical PED operating principle is shown in Fig. 1. Generation of the signal requires three basic functions:

1) Optical bit-rate filtering to suppress the label using an optical Q-filter such as a Fabry–Pérot (FP) filter or a laser with the proper bias, i.e., transparency. The Q-factor chosen should optimize the tradeoff between the rise/fall time and locking frequency, which affects the label suppression.
2) Optical envelope detection to generate an accurate envelope of the payload. This step should involve a threshold decision level for completing label removal. Examples include gain suppression in a laser, cross-gain modulation (XGM) in an SOA, or passing the signal through an SOA with limited bandwidth. In order to generate flat envelope signals in the presence of long sequences of zeros, a frequency response that is relatively slow compared to the packet bit duration is desired (see Section III).
3) Re-inversion of the envelope is required if the envelope generated in the previous step is inverted. This can be achieved by XGM in an SOA or gain suppression in a laser.

For Function 1, we use an SGDBR laser biased at transparency. To perform Function 2, we use gain suppression in a single-mode distributed Bragg reflector (DBR) LD. This LD provides thresholding and has a slow response relative to the

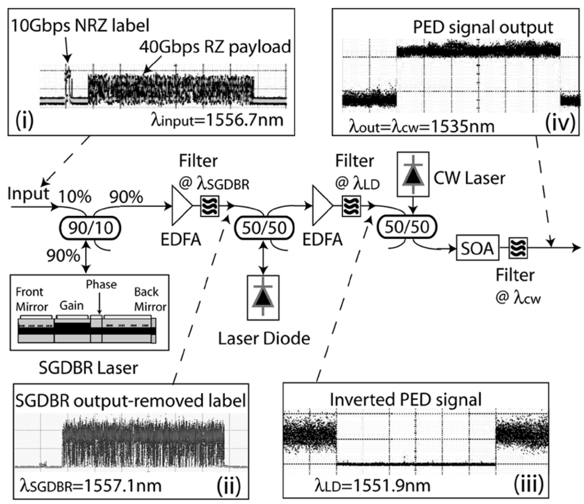

Fig. 2. Experimental setup with oscilloscope traces at various points in the PED circuit, labeled corresponding to Fig. 1.

bit duration, creating an inverted envelope of the payload. We then invert this signal for Function 3 using XGM in an SOA.

Our experimental setup is shown in Fig. 2. The SGDBR is biased near transparency and its mirrors and phase section are tuned so that the laser's effective length corresponds to a 40-GHz resonant frequency. Due to enhanced resonance at 40 GHz, the SGDBR lases or not depending on the input optical packets, as shown in Fig. 2 inset (i): lasing when the 40-Gb/s RZ payloads are present, but not when the 10-Gb/s NRZ labels enter. Thus, the laser acts as an optical Q-filter with a low Q-factor, resulting in fast rise/fall times. The SGDBR must also be tuned so that the input wavelength is within the range of the mirror reflectivity peaks. The SGDBR is finely tunable in wavelength over 70 nm, implying the input wavelength range could be very high. The SGDBR is polarization-dependent so a polarization controller is used before it.

The output of the SGDBR laser with suppressed optical label as shown in the inset picture (ii) in Fig. 2 goes back into the coupler and then goes to the DBR LD. The LD is biased above threshold at a level such that the SGDBR laser output can suppress its gain or not: the payload corresponding part in the SGDBR laser output can turn off the LD. Thus, the output of the LD is an inverted payload envelope signal shown as the inset picture (iii) in Fig. 2. The inverted PED signal is then inverted again to obtain a noninverted PED signal at another wavelength by using XGM in an SOA, as shown in the inset picture (iv) in Fig. 2. Thus, the PED signal can be at any desired wavelength other than λ_{LD}. Proper choice of this wavelength may improve XGM performance.

III. Theoretical Analysis and Discussion

To estimate the rise/fall time and amount of label suppression after the optical bit-rate filtering, we performed the following analysis based on the setup in Fig. 2. Most of this information can be obtained by first determining the Q-factor of the SGDBR laser. Details of this laser were reported in [6]. It has front and back mirrors, a gain section, and a phase section. For our operating conditions, the Q-factor is

$$Q = \frac{\tau_d}{T_{\text{RT}}} = \frac{f_0}{\Delta f_{\text{lock}}} \tag{1}$$

in which τ_d is the cavity decay time, T_{RT} is the cavity round-trip time, f_0 is the bit-rate frequency, and Δf_{lock} is the locking range. For a passive device (FP filter), the cavity decay time is the same as the photon lifetime τ_p [5]

$$\frac{1}{\tau_d} = \frac{1}{\tau_p} = v_g\left(\langle\alpha_i\rangle + \alpha_m\right). \tag{2}$$

v_g is the group velocity, $\langle\alpha_i\rangle$ is the average internal modal loss, and α_m is the mirror loss. The mirror loss is

$$\alpha_m = \frac{1}{L}\ln\left(\frac{1}{\sqrt{R_1 R_2}}\right). \tag{3}$$

L is the length of the laser cavity, and R_1 and R_2 are the power reflectivities of the laser's front and back mirrors, respectively. When gain is introduced to the laser, the cavity decay time equals the effective photon lifetime τ_p', given by [5]

$$\frac{1}{\tau_d} = \frac{1}{\tau_p'} = \frac{1}{\tau_p} - \Gamma v_g g \tag{4}$$

in which Γ is the confinement factor and g is is the gain. For a laser biased at transparency the modal gain. Γg is equal to the average internal loss. Then the cavity decay time simplifies to

$$\tau_d = \frac{1}{v_g \alpha_m}. \tag{5}$$

We estimate the reflectivities of the mirrors to be 0.5 and 0.7 based on data provided in [6]. The laser length is about 960 μm. Thus, the Q-factor is approximately 0.95 and the locking bandwidth is 42.2 GHz for 40-Gb/s operation. Outside the range of 40 Gb/s$\pm$21.1 GHz, all frequencies are significantly suppressed. As shown experimentally in Fig. 2(ii), labels are effectively removed because 10-Gb/s NRZ data is well outside of the locking range and further NRZ data has no clock tone. Label suppression is greater than 10 dB. The label location relative to the payload does not affect the PED performance because the optical bit-rate filtering process happens in the frequency domain. Rise/fall times can be found by a simple analysis of the power in the laser cavity as data is injected. We expect a 90/10 rise time of 4 bits assuming 50% mark ratio, and fall time of 2 bits. Equation (4) shows that if the gain is above transparency, the cavity decay time increases. Thus, a laser biased above transparency has higher Q and decreased locking bandwidth, suppressing labels even more and significantly increasing the rise/fall times.

Other components in the circuit should not affect the locking range of the circuit. However, the rise/fall times of the PED output will be significantly affected by these components. The processes of gain suppression and XGM are dependent on the

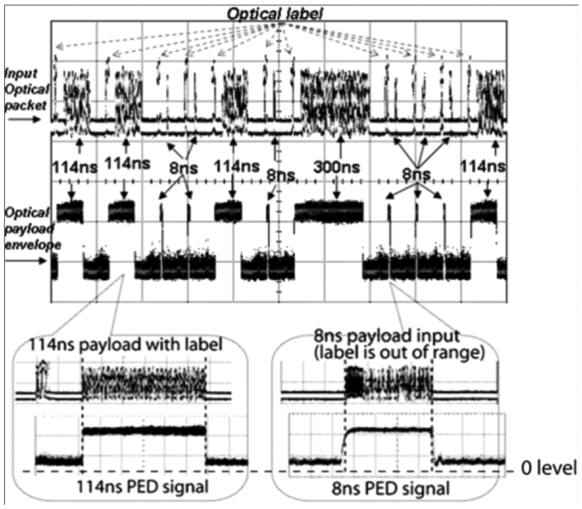

Fig. 3. Oscilloscope traces of optical packet input (top) and corresponding payload envelope signals (bottom) for variable length payloads with zooms of a 114-ns payload (left inset) and 8-ns payload (right inset).

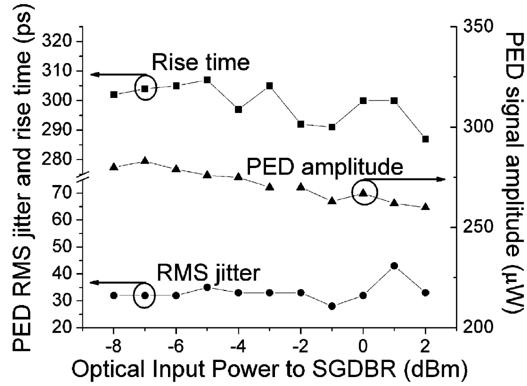

Fig. 4. PED jitter and rise time (left axis, with line break) and amplitude (right axis) versus input power to the SGDBR (after 90/10 coupler).

gain recovery time and bandwidth of the devices used. The devices should be slow compared to the payload bit rate since we do not want the laser or SOA to recover at any point during the duration of the payload. If the input payload contains long sequences of zeros, the optical bit-rate filtering process may see some dips but the subsequent envelope detection process with threshold function can minimize the effect and flatten the PED signal. In the worst case, the zero sequence in the payload is longer than the PED fall time (18 bits for our current setup) resulting in an unusable PED signal.

IV. Experimental Results

A repeating 60-packet-long IMIX (Internet mix) packet stream approximating Internet traffic was sent to the PED setup shown in Fig. 2: for every 12 packets there are 7×40 byte payloads (8 ns each), 4×570 byte payloads (114 ns each), and 1×1500 byte payload (300 ns each). At the transmitter, bits in each payload are predetermined by a random number generator and labels are defined by the user. Fig. 3 shows PED signals generated for variable length payloads with labels. Using an oscilloscope, we measured the PED signals' durations to be equal to the incoming payloads' durations, shown in Fig. 3 insets. Using an optical gate, this PED signal can erase labels while the payloads pass through. Alternatively, the inverted PED signal directly from the LD could erase the labels via XGM in an SOA, as done in [4].

We measured the rise time and rms jitter for a 10-dB dynamic range in input power to the SGDBR. Results are shown in Fig. 4. Typical results are a rise time of 300 ps and rms jitter of 30 ps. The input signal rise time is instantaneous and the input jitter is less than 1 ps. The PED signal amplitude is approximately 260 μW and the fall time is 450 ps for this dynamic range. The extinction ratio (ER) for the PED signal is 6.7 dB for an input signal ER of 10 dB. The ground level of the PED signal partly comes from the inherent optical emission of the DBR LD, partly from the relatively low ER of the XGM process in the SOA. In an optical gate with a nonlinear transfer function such as an SOA-based Mach–Zehnder interferometer [7], the label erasure ER could be over 20 dB using our PED signal.

V. Conclusion

We have demonstrated an all-optical PED technique for use in optical label swapping networks. Measurement and demonstration of the basic functions required for all-optical PED generation was described. The circuit is based on bit-rate filtering using a resonant laser biased near transparency to remove labels, followed by a gain suppressed laser to create an envelope of the payload only. The payload envelope signal has a rise time of 300 ps, fall time of 450 ps, and rms jitter in the rising and falling edges near 30 ps. The signal can be used to erase labels and to time the insertion of new labels. Compared to previous methods using electrical components [3] or optoelectronic components [4], the all-optical PED method achieves not only significant performance improvements but also the potential for monolithic integration of all-optical PED circuits.

References

[1] D. J. Blumenthal, B.-E. Olsson, G. Rossi, T. E. Dimmick, L. Rau, M. Masanovic, O. Lavrova, R. Doshi, O. Jerphagnon, J. E. Bowers, V. Kaman, L. A. Coldren, and J. Barton, "All-optical label swapping networks and technologies," *J. Lightw. Technol.*, vol. 18, no. 12, pp. 2058–2075, Dec. 2000.

[2] A. Viswanathan, N. Feldman, Z. Wang, and R. Callon, "Evolution of multiprotocol label switching," *IEEE Commun. Mag.*, vol. 36, no. 5, pp. 165–173, May 1998.

[3] Z. Hu, R. Doshi, H.-F. Chou, H. N. Poulsen, D. Wolfson, J. E. Bowers, and D. J. Blumenthal, "Optical label swapping using payload envelope detection circuits," *IEEE Photon. Technol. Lett.*, vol. 17, no. 7, pp. 1537–1539, Jul. 2005.

[4] B. R. Koch, Z. Hu, J. E. Bowers, and D. J. Blumenthal, "Integrated optical label read and payload envelope detection circuit for optical label swapping," in *Opt. Fiber Commun. Conf.*, 2006, Paper OWL7.

[5] L. A. Coldren and S. W. Corzine, *Diode Lasers and Photonic Integrated Circuits*. New York: Wiley, 1995, ch. 2, 5.

[6] Y. A. Akulova, G. A. Fish, P.-C. Koh, C. L. Schow, P. Kozodoy, A. P. Dahl, S. Nakagawa, M. C. Larson, M. P. Mack, T. A. Strand, C. W. Coldren, E. Hegblom, S. K. Penniman, T. Wipiejewski, and L. A. Coldren, "Widely tunable electroabsorption-modulated sampled-grating DBR laser transmitter," *IEEE J. Sel. Topics Quantum Electron.*, vol. 8, no. 6, pp. 1349–1357, Nov./Dec. 2002.

[7] S.-C. Cao and J. C. Cartledge, "Characterization of the chirp and intensity modulation properties of an SOA-MZI wavelength converter," *J. Lightw. Technol.*, vol. 20, no. 4, pp. 689–695, Apr. 2002.